npg

ORIGINAL ARTICLE

Thermopower enhancement in $Pb_{1-x}Mn_xTe$ alloys and its effect on thermoelectric efficiency

Yanzhong Pei[1], Heng Wang[2], Zachary M Gibbs[2], Aaron D LaLonde[2] and G Jeffrey Snyder[2]

The Seebeck coefficient of p-type PbTe can be enhanced at 300 K, either due to the addition of Tl-resonant states or by manipulation of the multiple valence bands by alloying with isovalent compounds, such as MgTe. PbTe alloyed with MnTe shows a similar thermopower enhancement that could be due to either mechanism. Here we investigate the characteristics that distinguish the resonant state mechanism from that due to multiple valence bands and their effect on the thermoelectric figure of merit, *zT*. Ultimately, we find that the transport properties of PbTe alloyed with MnTe can be explained by alloy scattering and multiple band model that result in a *zT* as high as 1.6 at 700 K, and additionally a ∼30% enhancement of the average *zT*.

INTRODUCTION

The efficiency of a thermoelectric converter is determined by the material's figure of merit, $zT = S^2 \sigma T/(\kappa_E + \kappa_L)$, where, S, σ, κ_E and κ_L are the Seebeck coefficient, electrical conductivity and the electronic and lattice components of the thermal conductivity ($\kappa = \kappa_E + \kappa_L$), respectively. Increasing the Seebeck coefficient is an obvious goal for obtaining high-efficiency thermoelectric materials, but other changes in transport properties, correlated with an increase in S may not ultimately lead to an improvement in zT.

A variety of strategies have been employed to achieve high zT in bulk thermoelectric PbTe, most recently by introducing resonant states through Tl doping[1,2] and by utilizing carriers from multiple bands.[3–6] Both approaches have been shown to result in an enhanced Seebeck coefficient as compared with that expected from the principal valence band.

Under certain carrier-scattering assumptions, the enhanced Seebeck coefficient can be well understood by a sharp increase in the local density of states around the Fermi level, which is also interpreted as an increased local density of states effective mass (m_d^*). However, the overall benefit of such an increase in Seebeck coefficient can be compensated by a decrease in mobility, because the increased local density of states usually leads to a heavier transport-effective mass of carriers. When the carriers are predominantly scattered by phonons, as has been found in most of the known and good high-temperature thermoelectrics, the following transport equations help understand how m_d^* affects zT.

According to nonpolar phonon-scattering theory,[7,8] and taking band nonparabolicity into account, the single Kane band model[9] (assuming an isotropic band for simplicity) provides the expressions for the transport coefficients[10,11] as follows:

Hall carrier concentration

$$n_H = \frac{1}{eR_H} = A^{-1} \frac{N_v(2m_b^* k_B T)^{3/2}}{3\pi^2 \hbar^3} {}^0F_0^{3/2}, A = \frac{{}^0F_{-4}^{1/2} \cdot {}^0F_0^{3/2}}{({}^0F_{-2}^1)^2} \quad (1)$$

Hall mobility

$$\mu_H = A \frac{2\pi \hbar^4 e C_l}{m_b^* 5/2 (2k_B T)^{3/2} E_{def}^2} \frac{3 {}^0F_{-2}^1}{{}^0F_0^{3/2}} \quad (2)$$

Seebeck coefficient

$$S = \frac{k_B}{e} \left[\frac{{}^1F_{-2}^1}{{}^0F_{-2}^1} - \xi \right] \quad (3)$$

and Lorenz number

$$L = \left(\frac{k_B}{e} \right)^2 \left[\frac{{}^2F_{-2}^1}{{}^0F_{-2}^1} - \left(\frac{{}^1F_{-2}^1}{{}^0F_{-2}^1} \right)^2 \right] \quad (4)$$

where ${}^nF_k^m$ has a similar form as the Fermi integral

$$ {}^nF_k^m = \int_0^\infty \left(-\frac{\partial f}{\partial \varepsilon} \right) \varepsilon^n (\varepsilon + \alpha \varepsilon^2)^m [(1 + 2\alpha \varepsilon)^2 + 2]^{k/2} d\varepsilon \quad (5)$$

In the above equations, R_H is the Hall coefficient, N_v the number of degenerated valleys for the band, m_b^* the effective mass for each

[1]School of Materials Science and Engineering, Tongji University, Shanghai, China and [2]Department of Materials Science, California Institute of Technology, Pasadena, CA, USA
Correspondence: Dr Y Pei, School of Materials Science and Engineering, Tongji University, 4800 Caoan Road, Shanghai 201804, China.
E-mail: peiyanzhong@gmail.com
or Dr GJ Snyder, Department of Materials Science, California Institute of Technology, Pasadena, CA 91125, USA.
E-mail: jsnyder@caltech.edu

valley, k_B the Boltzmann constant, $\hbar$ the reduced Planck constant, C_l the average longitudinal elastic moduli,[8,12] E_{def} the deformation potential coefficient[7,8] characterizing the effectiveness of nonpolar phonons to scatter charge carriers, ξ the reduced Fermi level, ε the reduced energy of the electron state, $\alpha(=k_BT/E_g)$ the reciprocal reduced band separation (E_g, at L point of the Brillouin zone in this study) and f the Fermi distribution. One obtains:

$$zT = \frac{[{}^1F^1_{-2}/{}^0F^1_{-2} - \xi]^2}{[{}^2F^1_{-2}/{}^0F^1_{-2} - ({}^1F^1_{-2}/{}^0F^1_{-2})^2] + B^{-1}(3{}^0F^1_{-2})^{-1}} \text{ with } B = \frac{N_v}{m_b^*\kappa_L}\frac{2k_B^2T\hbar C_l}{3\pi E_{def}^2}.$$

This equation demonstrates that increasing zT depends on achieving larger values of the B factor, first described by Chasmar and Stratton,[13] aside from tuning the carrier concentration to obtain optimized values for these integrals. Within this model, increasing the local density of states effective mass, $m_d^* = N_v^{2/3}m_b^*$, to increase the Seebeck coefficient through increasing m_b^* (that is, band flattening) actually *decreases* the B factor and therefore *lowers* zT.[13–17] However, increasing m_d^* through increasing the number of degenerate valleys would lead to an enhancement of zT.[3–5,18,19] Although this equation is exact for simple single-band conduction with nonpolar phonon scattering, it is a valuable guide for discovering, improving and explaining good thermoelectric materials.

It is not obvious how to increase the symmetry-related number of valleys in a given material. However, aligning multiple bands (even those without exactly the same band mass) within a few k_BT (k_B is the Boltzmann constant) around the Fermi level can be considered as an effective way to increase m_d^* to achieve useful enhancement on Seebeck coefficient.[3,5]

It is known that slightly (~ 0.2 eV) below the principal nonparabolic (light) valence band, there is effectively a heavier secondary parabolic valence band.[11,20–22] As the temperature increases, the light band reduces its energy and converges with the heavy band edge at $T \sim 450$ K,[11,20,23] whereas the energy for the heavy band remains roughly constant as measured from the conduction band edge. This two-valence band model is used in the following discussion because it describes experimental results sufficiently well and facilitates predictive modeling.[3–6,11,18,21–30] Note that band-structure calculations indicate a complex Fermi surface, rather than two simple bands, that predicts a qualitatively similar Seebeck coefficient at low carrier concentrations ($<10^{19}$ cm^{-3}).[31]

Additionally, alloys of PbTe with isovalent elements can also adjust the energy offset between the two-valence bands leading to similar band-tuning effects.[3,5,29,32–40] In the case of $Pb_{1-x}Mg_xTe$, the room-temperature band gap increases with increasing Mg content, meaning the energy of the light valence band is reduced to achieve an effective alignment with the heavy band even at room temperature.[5,33–35] This is an opposite effect to the $PbTe_{1-x}Se_x$ alloys, which has a slightly lower band gap that produces band alignment at higher temperatures.[3] Such alloying also leads to alloy scattering of phonons, which reduces the lattice thermal conductivity and is helpful for high zT.[3,5,6,29,41]

Tl-doped PbTe exhibits unique transport behavior,[42–47] such as superconductivity[45] and unusual optical properties,[48] presumably due to the resonant states that form. Such resonant state effects are not expected in isovalent alloys of MgTe or PbSe.[2]

Alloying of PbTe with MnTe also modifies the band structure[38–40] and therefore the transport properties.[32,37] It is not entirely clear whether Mn is electrically inactive[2] that only leads to small adjustments of the band energies (as has been assumed for PbSe and MgTe alloys), or whether transport property modifications are due to a resonant state effect from the possible multiple valencies in Mn compounds. Other 3d transition metals, such as Ti[49–52] and

Cr,[52–54] exhibit resonant state effects in PbTe. It also should be noted that d-resonant states are believed to be less favorable than s- or p-states for improving zT of semiconductors.[2]

$Pb_{1-x}Mn_xTe$ with Na doping (p-type) was intensively studied with a focus on the room-temperature transport properties;[37] yet, the high-temperature thermoelectric performance was not evaluated systematically. Mn–Pb–Sn–Te alloys known as '3P-PbTe'[55] were used for National Aeronautics and Space Administration space mission for several decades, however, the detailed composition and transport properties are not well publicized.

In this paper, we achieved an enhanced Seebeck coefficient in PbTe, particularly near room temperature, through alloying with MnTe. The data are directly compared with the Tl- and Mg-alloyed material systems having similar behavior but due to different mechanisms. The Mn alloys behave similarly to the Mg alloys as opposed to Tl alloys, suggesting that the mechanism is by adjustment of band energies rather than resonant states.[5,29,32,36–38]

MATERIALS AND METHODS

$Pb_{1-x}Mn_xTe$ alloys with x up to 0.15 were synthesized using melting, quenching, annealing and hot-pressing methods. To make direct comparisons with literature,[37] compositions with $x = 0.03$–0.04 were focused on in this study and Na doping was used to tune the carrier concentration for high-thermoelectric performance over the entire temperature range. Detailed synthesis and measurements on transport properties can be found in our previous reports.[3,4] The optical band gap was measured on undoped samples using diffuse reflectance spectroscopy (Nicolet 6700 FTIR (Harrick Scientific, Pleasantville, NY, USA) with Praying Mantis attachment). It should be noted that the heat capacity was determined from the measured values of Blachnik[56] by $C_p(k_B/atom) = (3.07 + 0.00047(T/K - 300))$, which is typically used for lead chalcogenides.[3,4,18,30,56–59] The relative measurement uncertainty for each transport property (S, σ and κ) is about 5% because most measurements are performed on the same instruments. The obtained lattice parameter followed a Vegard's law relationship when $x < \sim 0.1$ and saturated when $x > \sim 0.1$, which agrees well with the literature results[37] and indicates a solubility of $\sim 10\%$. This is also confirmed by scanning electron microscopy, showing MnTe precipitates in samples with $x > \sim 0.1$.

RESULTS AND DISCUSSION

Comparisons of the transport properties among PbTe:Na,[24,26,37,42,45] $Pb_{1-x}Mn_xTe$:Na,[37] $Pb_{1-x}Mg_xTe$:Na[5] and PbTe:Tl[42,45,48] are shown in Figure 1. The current work shows good agreement with the literature results. It is shown that alloying PbTe with MnTe and MgTe has undistinguishable Seebeck coefficient and Hall mobility, suggesting a similar effect on modifying the band structure.[5,32–38] This can be understood by the undistinguishable alloy composition-dependent direct optical band gap (E_g) in these two alloy systems as shown in Figure 2. This is also consistent with the band-structure calculation in $Pb_{1-x}Mn_xTe$.[40] The beneficial effect of band-structure modification on the thermoelectric properties in $Pb_{1-x}Mg_xTe$:Na has been shown previously.[5]

The observed enhancement (flattening) of the Seebeck coefficient (S) in PbTe:Na at high carrier concentrations ($n_H > 4 \times 10^{19}$ cm^{-3}) has been attributed to the redistribution of carriers between the light and heavy hole bands at these doping levels.[4,5,11,24,26] Alloying with MnTe leads to a similar S enhancement observed at lower carrier concentrations ($n_H > 1 \times 10^{19}$ cm^{-3}). This can be ascribed to the large carrier population from the heavy-mass hole band, resulting from the decrease of the energy offset between light and heavy hole bands,[32,37,40] meaning an increased m_d^* through multiple band conduction (an increase in N_v). Transport properties, including[37] Seebeck coefficient, change monotonously with increasing MnTe
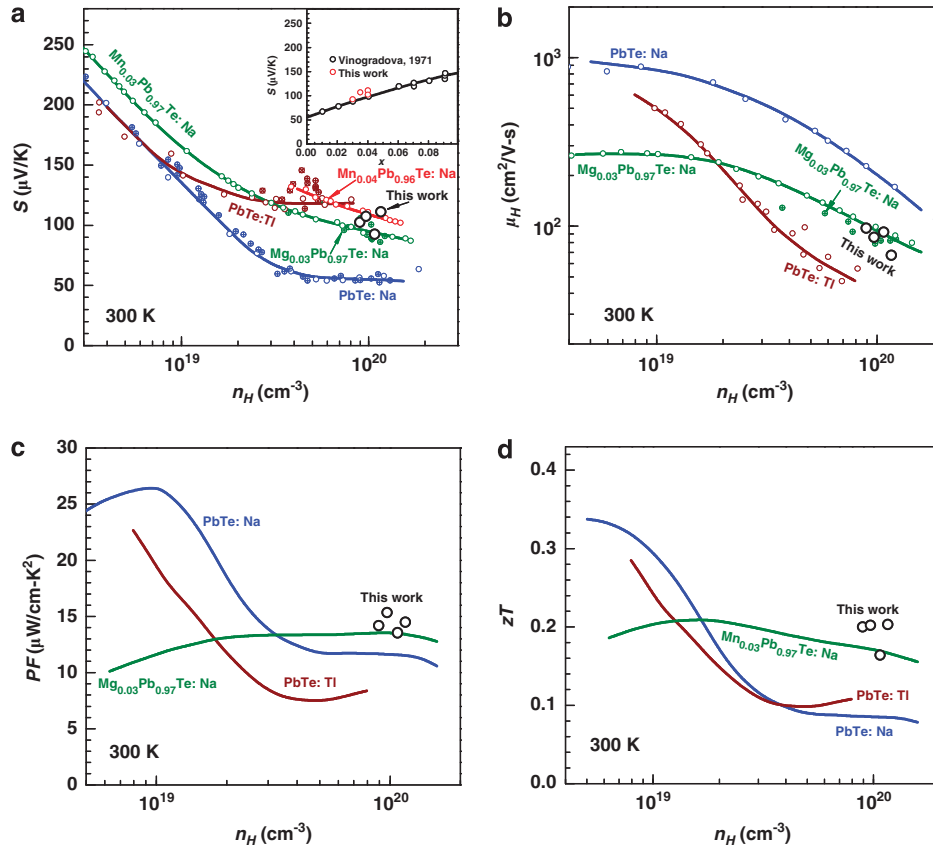
Figure 1 Room temperature Hall carrier concentration-dependent Seebeck coefficient (**a**), Hall mobility (**b**), power factor (**c**) and figure of merit (**d**) for PbTe:Na, PbTe:Tl and $Pb_{1-x}Mn_xTe$:Na/$Pb_{1-x}Mg_xTe$:Na at room temperature. The inset shows the alloy composition-dependent Seebeck coefficient at room temperature for $Pb_{1-x}Mn_xTe$:Na having similar carrier concentration. Both band-structure modification due to alloying and resonant states enhance Seebeck coefficient at the expense of reducing the Hall mobility, but the band-modification effect eventually leads to an enhancement on zT at $n_H > 5 \times 10^{19}\,cm^{-3}$, resulting in optimized p-PbTe materials for thermoelectric applications at elevated temperatures.

content (inset of Figure 1a) because of the gradual modification of the band structure. Small deviation between current and literature work can be ascribed to the slight difference in the carrier concentration. The observed S enhancement at low carrier concentrations ($n_H < 1 \times 10^{19}\,cm^{-3}$) is due to the increase of the effective mass for the light band itself originating from the increased band gap (Figure 2, gap between light valence and conduction bands, L point in the Brillouin zone) in this alloy system having Kane-type nonparabolic bands.

PbTe:Tl, in contrast to $Pb_{1-x}Mn_xTe$:Na and $Pb_{1-x}Mg_xTe$:Na, has an increased m_d^* due to either a band flattening[2,47,60] or an additional piece of the Fermi surface.[61] In the case of the latter, a similar effect with increasing N_v can be expected, providing a suitable Fermi level. The Tl-resonant states result in an S enhancement only at high doping levels ($n_H > 1 \times 10^{19}\,cm^{-3}$). When $n_H > 2 \times 10^{19}\,cm^{-3}$, the comparable Seebeck coefficient for PbTe:Tl and $Pb_{1-x}Mn_xTe$:Na with $x = 0.03$–0.04 indicates a similar m_d^* for both materials.

It is normally expected that an increased m_d^*, particularly due to an increase on m_b^* (band flattening) leads to a significant reduction on the mobility (Equation 2).[16] According to Kane band theory,[9] a roughly 15% increased band gap in $Pb_{1-x}Mn_xTe$ ($x = 0.03$–0.04)[38] would lead to an increase on m_b^* for the light band by approximately the same degree. As a result, a ~40% reduction (Equation 2) on the Hall mobility (μ_H) is expected in the single band-conduction region ($n_H < 1 \times 10^{19}\,cm^{-3}$). The observed further reduction on
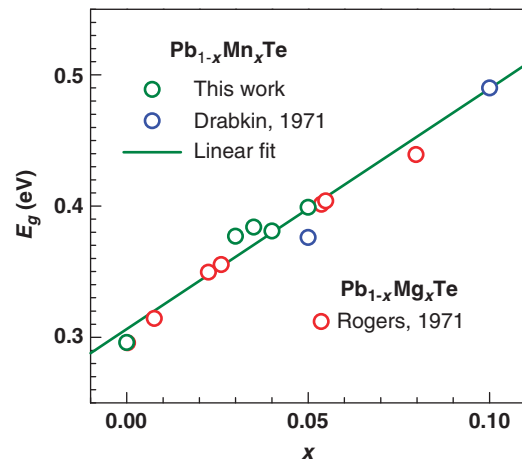

Figure 2 Direct optical band gap (E_g) as a function of alloy composition for $Pb_{1-x}Mn_xTe$ and $Pb_{1-x}Mg_xTe$ at room temperature.

μ_H in $Pb_{1-x}Mn_xTe$ at these doping levels is presumably due to the additional scattering by alloy defects and other scattering sources.[62,63] The reduced μ_H at $n_H > 1 \times 10^{19}\,cm^{-3}$ can be understood by a larger fraction of carriers attributed to the low-mobility heavy hole band, as compared with PbTe:Na.

In PbTe:Tl, a significant reduction on μ_H is observed at high doping levels ($n_H > 2 \times 10^{19}$ cm^{-3}), being much lower than that in Pb$_{1-x}$Mn$_x$Te:Na or Pb$_{1-x}$Mg$_x$Te:Na, although the m_d^* values are comparable ($x = 0.03$–0.04 at similar doping levels). In a simplified one or two valence band model, this would indicate that the m_d^*-enhancement in PbTe:Tl is due to an increased m_b^* (that is, band flattening)[2,47,60] for the high Seebeck coefficient, rather than an increase in N_v from new carrier pockets (assuming an unchanged scattering mechanism).[1]

Equations (1–3) also leads to an expression for the power factor ($S^2\sigma = 3B\kappa_L^0 F_{-2}^1 ({}^1F_{-2}/{}^0F_{-2} - \xi)^2 /T$), indicating that higher values of the B factor are favorable. Increased m_b^* of the light valence band due to the widening of the band gap by alloying significantly reduces μ_H (Equation 2) and therefore the power factor[16] in Pb$_{1-x}$Mn$_x$Te:Na when $n_H < 1 \times 10^{19}$ cm^{-3}. In this carrier-concentration range, the transport properties are dominated by the light band. However, an enhancement on the power factor can be achieved due to a larger B factor by an effective increase of N_v in the alloy when $n_H > 5 \times 10^{19}$ cm^{-3}, where optimized thermoelectric performance can be obtained for p-PbTe materials over the entire temperature range.[3,4] On the other hand, PbTe:Tl shows little enhancement on power factor at any doping level. When all of the effects related to the enhanced Seebeck coefficient ($n_H > \sim 1 \times 10^{19}$ cm^{-3}) are taken into account, including the electronic thermal conductivity, significant enhancement of the figure of merit (Figure 1d) at 300 K compared with PbTe:Na is achieved in Pb$_{1-x}$Mn$_x$Te:Na. It is found that PbTe:Tl does not provide a substantial improvement compared with PbTe:Na at these temperatures despite having a similar Seebeck coefficient enhancement as found in Pb$_{1-x}$Mn$_x$Te:Na/Pb$_{1-x}$Mg$_x$Te:Na. The above

discussion is consistent with the recent theoretical work,[64] suggesting that an increase in N_v from new carrier pockets by resonant states are more favorable for thermoelectrics than an increase in m_b^* (band flattening).

A somewhat different explanation for the enhanced Seebeck coefficient of PbTe:Tl involves resonant scattering as opposed to changes in the density of states only. Resonant scattering from the resonant impurities are proposed to cause a strong energy-dependent relaxation time of carriers,[2,44,45,65] with a peak in scattering at the energy of the resonant states. If the Fermi level (E_F) and the resonant states (E_R) are positioned, such that the low-energy carriers are preferentially scattered, then there will be a thermopower enhancement. This explanation was given earlier for the enhanced Seebeck coefficient (and enhanced zT) in degenerate systems ($E_F > E_R$),[65] particularly in Tl and Na co-doped PbTe materials.[44,66] Such a mechanism may explain the enhancement of zT in PbTe:Tl at the highest doping levels (Figure 1d) and enable further improvement of zT in co-doped samples.

Alternatively, the preferential obstruction of the low-energy carriers (by their mobility reduction) can occur by a reduction in their velocity (or increase in effective mass) without altering the scattering mechanism.[13–17] If the resonant states indeed cause the bands to flatten (large m_b^*) in a narrow energy targeting the low-energy carriers, the Seebeck coefficient could be enhanced while maintaining a nonpolar phonon-scattering mechanism (as observed in PbTe:Tl by Nernst effect measurement).[1]

The enhanced Seebeck coefficient in Pb$_{1-x}$Mn$_x$Te:Na and PbTe:Tl can also be found at high temperatures, accompanied by an increased resistivity due to the lower mobility (Figure 3). The similar transport
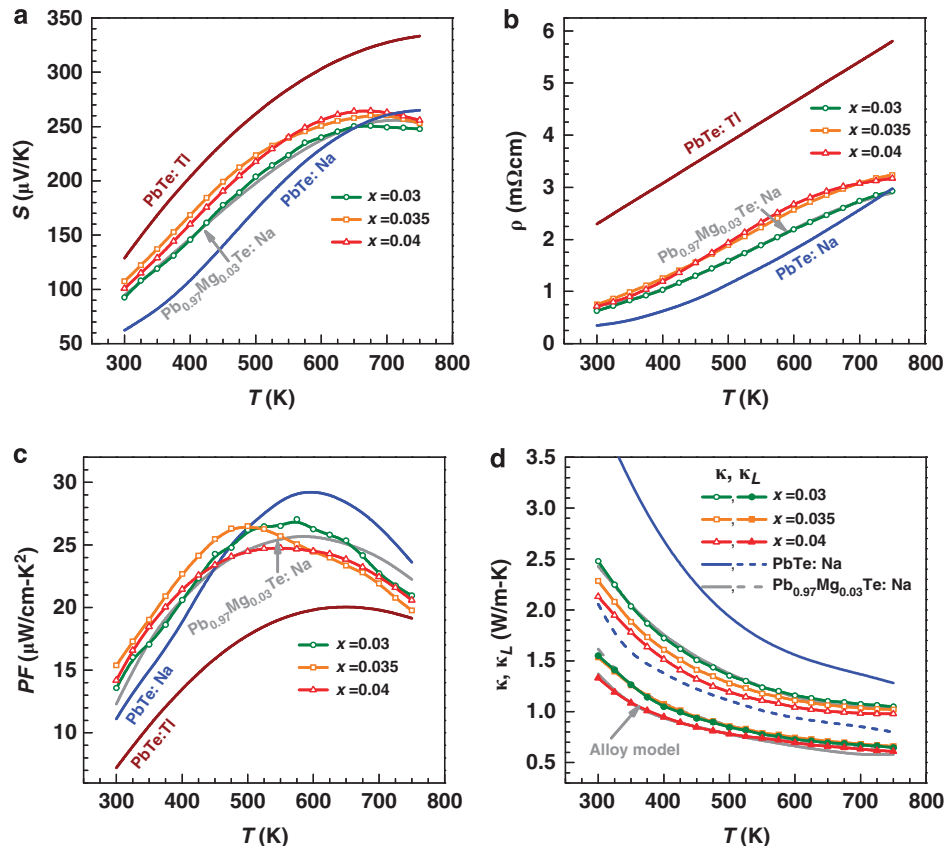

Figure 3 Temperature-dependent Seebeck coefficient (**a**), resistivity (**b**), power factor (**c**) and thermal conductivity (**d**) for PbTe:Na, PbTe:Tl, Pb$_{1-x}$Mn$_x$Te:Na and Pb$_{0.97}$Mg$_{0.03}$Te:Na. The reduced lattice thermal conductivity (**d**) can be attributed to alloy-scattering Pb$_{1-x}$Mn$_x$Te:Na.

properties of $Pb_{0.97}Mn_{0.03}Te$ and $Pb_{0.97}Mg_{0.03}Te$ having similar carrier concentration are also shown in this figure, indicating that these have a similar band-structure modification. Because the light hole band continuously reduces its energy and is eventually supposed to have energy below that of the heavy hole band at high temperatures, one would expect a gradual weakening of the multiple band-conduction effect in $Pb_{1-x}Mn_xTe$:Na as compared with PbTe:Na at high temperatures. This effect is seen in Figure 3c where the power factor of $Pb_{1-x}Mn_xTe$:Na becomes less than that of PbTe:Na at $T > \sim 450$K. PbTe:Tl does not show such behavior in either the Seebeck or the power factor at any temperature, further indicating that the increased m_d^* is due to a different mechanism.[2,47,60]

The enhanced Seebeck coefficient of $Pb_{1-x}Mn_xTe$:Na at low electrical conductivity leads to a low electronic contribution to the thermal conductivity while maintaining a high power factor comparable to PbTe:Na. In addition, it is expected that the lattice thermal conductivity (κ_L) can be reduced through phonon scattering by mass and strain contrasts in the alloy.[41,67–69] The observed κ_L reduction can be explained well by the Debye–Callaway model[67–69] as has previously been found in other PbTe alloys.[3,70–72] In this way, the total thermal conductivity (κ) is substantially reduced in $Pb_{1-x}Mn_xTe$:Na alloys as shown in Figure 3d.

Despite the similarly high Seebeck coefficient in $Pb_{1-x}Mn_xTe$:Na and PbTe:Tl, the different mobility leads to different net results on the figure of merit as shown in Figure 4. $Pb_{1-x}Mn_xTe$:Na shows a great enhancement on zT over the entire temperature range compared with PbTe:Na, which can be understood by the multiple band-conduction mechanism at low temperatures and reduced lattice thermal conductivity at high temperatures.[5] Although in PbTe:Tl, the enhancement of the Seebeck coefficient is largely compensated by the reduced mobility and therefore leads to a comparable zT with PbTe:Na. Quantitatively, the total effect of alloying PbTe with MnTe leads to $\sim 30\%$ enhancement on average zT in the temperature range studied here and similar to that found in $Pb_{1-x}Mg_xTe$:Na.[5]
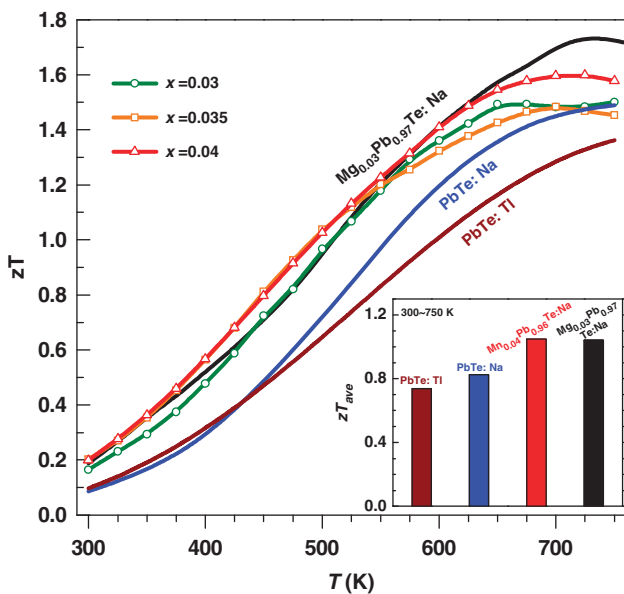
In summary, we demonstrate that the enhanced Seebeck coefficient in $Pb_{1-x}Mn_xTe$:Na is most likely due to the same multiple band-conduction mechanism found in $Pb_{1-x}Mg_xTe$:Na, as opposed to resonant states observed in PbTe:Tl. Alloying PbTe with MnTe increases the figure of merit at low temperatures and provides the additional advantage of alloy scattering leading to high zT at high temperatures. A peak zT as high as 1.6 and $\sim 30\%$ enhancement on the average zT over the entire temperature range emphasize the effectiveness of alloying to tune the multiple band conduction (large N_v) and further supports this approach in the search of high-efficiency thermoelectric materials.

ACKNOWLEDGEMENTS

1   Heremans, J. P., Jovovic, V., Toberer, E. S., Saramat, A., Kurosaki, K., Charoenphakdee, A., Yamanaka, S. & Snyder, G. J. Enhancement of thermoelectric efficiency in PbTe by distortion of the electronic density of states. *Science* **321**, 554–557 (2008).

2   Heremans, J. P., Wiendlocha, B. & Chamoire, A. M. Resonant levels in bulk thermoelectric semiconductors. *Energ. Environ. Sci.* **5**, 5510–5530 (2012).

3   Pei, Y., Shi, X., LaLonde, A., Wang, H., Chen, L. & Snyder, G. J. Convergence of electronic bands for high performance bulk thermoelectrics. *Nature* **473**, 66–69 (2011).

4   Pei, Y., LaLonde, A., Iwanaga, S. & Snyder, G. J. High thermoelectric figure of merit in heavy-hole dominated PbTe. *Energ. Environ. Sci.* **4**, 2085–2089 (2011).

5   Pei, Y., LaLonde, A. D., Heinz, N. A., Shi, X., Iwanaga, S., Wang, H., Chen, L. & Snyder, G. J. Stabilizing the optimal carrier concentration for high thermoelectric efficiency. *Adv. Mater.* **23**, 5674–5678 (2011).

6   LaLonde, A. D., Pei, Y., Wang, H. & Jeffrey Snyder, G. Lead telluride alloy thermoelectrics. *Mater. Today* **14**, 526–532 (2011).

7   Bardeen, J. & Shockley, W. Deformation potentials and mobilities in non-polar crystals. *Phys. Rev.* **80**, 72–80 (1950).

8   Herring, C. & Vogt, E. Transport and deformation potential theory for many-valley semiconductors with anisotropic scattering. *Phys. Rev.* **101**, 944–961 (1956).

9   Kane, E. Band structure of indium antimonide. *J. Phys. Chem. Solids* **1**, 249–261 (1957).

10 Ravich, Y. I., Efimova, B. A. & Tamarche, V. I. Scattering of current carriers and transport phenomena in Lead Chalcogenides.1. Theory. *Phys. Status Solidi B-Basic Res.* **43**, 11–33 (1971).

11 Ravich, Y. I., Efimova, B. A. & Smirnov, I. A. *Semiconducting Lead Chalcogenides* (Plenum Press, New York, 1970).

12 Lawaetz, P. Low-Field mobility and galvanomagnetic properties of holes in germanium with phonon scattering. *Phys. Rev.* **174**, 867–880 (1968).

13 Chasmar, R. P. & Stratton, R. The thermoelectric figure of merit and its relation to thermoelectric generators. *J. Electr. Control* **7**, 52–72 (1959).

14 Ure, R. W. & Heikes, R. R. In: *Thermoelectricity: Science and Engineering* (eds Heikes, R. R.& Ure, R. W.) Ch. 11, 339–388 (Interscience Publishers, New York, 1961).

15 Goldsmid, H. J. *Thermoelectric Refrigeration* (Plenum Press, New York, 1964).

16 Pei, Y., LaLonde, A. D., Wang, H. & Snyder, G. J. Low Effective mass leading to high thermoelectric performance. *Energ. Environ. Sci.* **5**, 7963–7969 (2012).

17 LaLonde, A. D., Pei, Y. & Snyder, G. J. Reevaluation of PbTe1-xIx as high performance n-type thermoelectric material. *Energ. Environ. Sci.* **4**, 2090–2096 (2011).

18 Wang, H., Pei, Y., LaLonde, A. D. & Snyder, G. J. Heavily doped p-Type PbSe with high thermoelectric performance: an alternative for PbTe. *Adv. Mater.* **23**, 1366–1370 (2011).

19 Fedorov, M. I. Band structure parameters influence on the thermoelectric figure of merit. *ECT2007. 5th European Conference on Thermoelectrics* **7**, 1–6 (2006).

20 Andreev, A. A. & Radionov, V. N. Determination of band structure of lead telluride from measurements of Hall effect at high temperatures. *Soviet Phys. Semiconductors* **1**, 145–148 (1967).

21 Allgaier, R. S. Valence Bands in Lead Telluride. *J. Appl. Phys.* **32**, 2185–2189 (1961).

22 Crocker, A. J. & Rogers, L. M. Valence band structure of PbTe. *J. Phys. Colloques* **29**, 129–132 (1968).

23 Kim, H. & Kaviany, M. Effect of thermal disorder on high figure of merit in PbTe. *Phys. Rev. B.* **86**, 045213 (2012).

24 Chernik, I. A., Kaidanov, V. I., Vinogradova, M. I. & Kolomoets, N. V. Investigation of the valence band of lead telluride using transport phenomena. *Soviet Phys. Semiconductors* **2**, 645–651 (1968).

25 Crocker, A. J. & Rogers, L. M. Interpretation of the Hall coefficient, electrical resisiivity anad Seebeckc oefficient of p-type lead telluride. *Brit. J. Appl. Phys.* **18**, 563–573 (1967).

Figure 4 Temperature-dependent figure of merit (zT) for PbTe:Na, PbTe:Tl, $Pb_{0.97}Mg_{0.03}Te$:Na and $Pb_{1-x}Mn_xTe$:Na, all calculated using the heat capacity of Blachnik.[56] Much like $Pb_{1-x}Mg_xTe$:Na,[5] the $Pb_{1-x}Mn_xTe$:Na alloy has $\sim 30\%$ greater average zT (inset) in the temperature range studied.

26 Airapetyants, S. V., Vinograd, M. N., Dubrovsk, I. N., Kolomoet, N. V. & Rudnik, I. M. Structure of the valence band of heavily doped lead telluride. *Soviet. Phys. Solid State* **8,** 1069–1072 (1966).

27 Sysoeva, L. M., Vinograd, M. N., Kolomoet, N. V. & Ravich, Y. I. Influence of the second valence band on the thermoelectric figure of merit of P-Type material. *Soviet Phys. Semiconductors* **3,** 975–977 (1970).

28 Allgaier, R. S. & Houston, B. B. Hall coefficient behavior and the second valence band in lead telluride. *J. Appl. Phys.* **37,** 302–309 (1966).

29 Pei, Y., LaLonde, A. D., Heinz, N. A. & Snyder, G. J. High Thermoelectric Figure of Merit in PbTe Alloys Demonstrated in PbTe–CdTe. *Adv. Energ. Mater.* **2,** 670–675 (2012).

30 Pei, Y., Heinz, N. A., LaLonde, A. & Snyder, G. J. Combination of large nanostructures and complex band structure for high performance thermoelectric lead telluride. *Energ. Environ. Sci.* **4,** 3640–3645 (2011).

31 Singh, D. J. Doping-dependent thermopower of PbTe from Boltzmann transport calculations. *Phys. Rev. B* **81,** 195217 (2010).

32 Osinniy, V., Jedrzejczak, A., Domuchowski, W., Dybko, K., Witkowska, B. & Story, T. Pb1-xMnxTe crystals as a new thermoelectric material. *Acta Phys. Pol. A* **108,** 809–816 (2005).

33 Rogers, L. & Crocker, A. Transport and optical properties of the CdxPb1-xSe and MgxPb1-xSe. *J. Phys. D Appl. Phys.* **5,** 1671 (1972).

34 Crocker, A. J. & Sealy, B. J. Some physical properties of PbTe-MgTe alloy system. *J. Phys. Chem. Solids* **33,** 2183–2190 (1972).

35 Rogers, L. M. & Crocker, A. J. Transport and optical properties of the MgxPbl-x,Te alloy system. *J. Phys. D Appl. Phys.* **4,** 1016 (1971).

36 Agaev, Z. F., Allakhverdiev, E. M., Murtuzov, G. M. & Abdinov, D. S. Electrical properties of Pb1-xMnxTe crystals. *Inorg. Mater.* **39,** 449–451 (2003).

37 Vinogradova, M. N., Kolomoets, N. V. & Sysoeva, L. M. Influence of manganese on energy spectrum of p-Pbte. *Soviet Phys. Semiconductors* **5,** 186–189 (1971).

38 Drabkin, I. A., Zakharyu, Gf & Nelson, I. V. Optical width of the forbidden band of Pb1-xMnxTe solid solutions. *Soviet Phys. Semiconductors* **5,** 277–278 (1971).

39 Neuwirth, J., Jantsch, W., Palmetshofer, L. & Zulehner, W. Optical properties of Pb 1-x Mn x Te. *J. Phys. C: Solid State Phys.* **19,** 2475 (1986).

40 Łusakowski, A., Bogusławski, P. & Radzyński, T. Calculated electronic structure of Pb1-xMnxTe (0<x<11%): the role of L and Σ valence band maxima. *Phys. Rev. B* **83,** 115206 (2011).

41 Pei, Y. & Morelli, D. Vacancy phonon scattering in thermoelectric In2Te3-InSb solid solutions. *Appl. Phys. Lett.* **94,** 122112 (2009).

42 Gruzinov, B., Drabkin, I. A., Eliseeva, Y., Lev, E. & Nelson, I. Electrical and optical properties of thallium-doped PbTe. *Soviet Phys. Semiconductors* **13,** 767–770 (1979).

43 Kaidanov, V. I., Nemov, S. A., Ravich, Y. I. & Zaitsev, A. M. Influence of resonance states on the hall-effect and electrical-conductivity of pbte doped with both thallium and sodium simultaneously. *Soviet Phys. Semiconductors* **17,** 1027–1030 (1983).

44 Kaidanov, V. I., Nemov, S. A. & Ravich, Y. I. Resonant scattering of carriers in Iv-Vi semiconductors. *Soviet Phys. Semiconductors* **26,** 113–125 (1992).

45 Nemov, S. A. & Ravich, Y. I. Thallium-doped lead chalcogenides: investigation methods and properties. *Usp Fiz Nauk+* **168,** 817–842 (1998).

46 Kaidanov & Ravich, Y. I. Deep and resonance states in AIV BVI semiconductors. *Usp Fiz Nauk+* **145,** 51–86 (1985).

47 Volkov, B., Ryabova, L. & Khokhlov, D. Mixed-valence impurities in lead telluride-based solid solutions—Resonant. *Phys. Uspekhi* **45,** 819–846 (2002).

48 Veis, A. N., Kaidanov, V. I., Nemov, S. A., Emelin, S. N., Ksendzov, A. Y. & Shalabutov, Y. K. Impurity states of thallium in lead telluride. *Soviet Phys. Semiconductors* **13,** 106–107 (1979).

49 Vinogradova, M. N., Gurieva, E. A., Zharskii, V. I., Zarubo, S. V. & Prokofeva, L. V. Influence of transition element (Ti) impurities on transport properties of PbTe.pdf. *Soviet Phys. Semiconductors* **12,** 387–390 (1978).

50 Sizov, F., Teterkin, V., Prokofeva, L. & Gurieva, E. Influence of a transition element impurity (Ti) on the energy band spectrum of PbTe. *Soviet Phys. Semiconductors* **14,** 1063–1064 (1980).

51 Koenig, J., Nielsen, M., Gao, Y.-B., Winkler, M. & Jacquot, A. Titanium forms a resonant level in the conduction band of PbTe. *Physical Rev. B Condensed Matter Mater. Phys.* **84,** 205126 (2011).

52 Teterkin, V. V., Sizov, F. F., Prokofeva, L. V., Gromovoi, Y. S. & Vinogradova, M. N. Resonance states of transition element (Ti, Cr) impurities in Pbte. *Soviet Phys. Semiconductors* **17,** 489–491 (1983).

53 Nielsen, M. D., Levin, E. M., Jaworski, C. M., Schmidt-Rohr, K. & Heremans, J. P. Chromium as resonant donor impurity in PbTe. *Phys. Rev. B* **85,** 045210 (2012).

54 Baleva, M. I. & Borissova, L. D. Optical-absorption in Pbte doped with Cr. *J. Phys. C Solid State* **16,** L907–L911 (1983).

55 Skrabek, E. A. & Trimmer, D. S. In: *CRC Handbook of Thermoelectrics* (ed. Rowe, D. M. 272 CRC Press, Boca Raton, FL, 1995).

56 Blachnik, R. & Igel, R. Thermodynamic Properties of IV-VI Compounds Lead Chalcogenides. *Z Naturforsch B* **29,** 625–629 (1974).

57 Pei, Y., May, A. F. & Snyder, G. J. Self-tuning the carrier concentration of PbTe/Ag2Te composites with excess ag for high thermoelectric performance. *Advan. Energ. Mater.* **1,** 291–296 (2011).

58 Zhang, Q., Wang, H., Liu, W., Wang, H., Yu, B., Zhang, Q., Tian, Z., Ni, G., Lee, S., Esfarjani, K., Chen, G. & Ren, Z. Enhancement of thermoelectric figure-of-merit by resonant states of aluminium doping in lead selenide. *Energ. Environ. Sci.* **5,** 5246–5251 (2012).

59 Pei, Y.-L. & Liu, Y. Electrical and thermal transport properties of Pb-based chalcogenides: PbTe, PbSe, and PbS. *J. Alloy Compd.* **514,** 40–44 (2012).

60 Ahmad, S., Hoang, K. & Mahanti, S. D. Ab initio study of deep defect states in narrow band-gap semiconductors: Group III impurities in PbTe. *Phys. Rev. Lett.* **96,** 056403 (2006).

61 Nakayama, K., Sato, T., Takahashi, T. & Murakami, H. Doping induced evolution of fermi surface in low carrier superconductor Tl-doped PbTe. *Phys. Rev. Lett.* **100,** 227004 (2008).

62 Pifer, J. H. Magnetic resonance of Mn2+ in PbS PbSe and PbTe. *Phys. Rev.* **157,** 272–276 (1967).

63 Brown, S. R., Toberer, E. S., Ikeda, T., Cox, C. A., Gascoin, F., Kauzlarich, S. M. & Snyder, G. J. Improved Thermoelectric Performance in Yb14Mn1−xZnxSb11 by the reduction of spin-disorder scattering. *Chem. Mater.* **20,** 3412–3419 (2008).

64 Cornett, J. E. & Rabin, O. Thermoelectric figure of merit calculations for semiconducting nanowires. *Appl. Phys. Lett.* **98,** 182104 (2011).

65 Ravich, Y. I. In: *CRC Handbook of Thermoelectrics* (ed. Rowe, D. M.) Ch. 7, 65–71 (CRC Press, Boca Raton, FL, 1995).

66 Jaworski, C. M., Wiendlocha, B., Jovovic, V. & Heremans, J. P. Combining alloy scattering of phonons and resonant electronic levels to reach a high thermoelectric figure of merit in PbTeSe and PbTeS alloys. *Energ. Environ. Sci.* **4,** 4155–4162 (2011).

67 Klemens, P. G. The scattering of low-frequency lattice waves by static imperfections. *Proc. Phys. Soc.* **A68,** 1113–1128 (1955).

68 Callaway, J. & Vonbaeyer, H. C. Effect of point imperfections on lattice thermal conductivity. *Phys. Rev.* **120,** 1149–1154 (1960).

69 Abeles, B. Lattice thermal conductivity of disordered semiconductor alloys at high temperatures. *Phys. Rev.* **131,** 1906–1911 (1963).

70 Alekseeva, G. T., Efimova, B., Ostrovsk, L. M., Serebrya, O. S. & Tsypin, M. Thermal conducitivty of solid solutions based on lead telluride. *Soviet Phys. Semiconductors* **4,** 1122–1125 (1971).

71 Koh, Y. K., Vineis, C. J., Calawa, S. D., Walsh, M. P. & Cahill, D. G. Lattice thermal conductivity of nanostructured thermoelectric materials based on PbTe. *Appl. Phys. Lett.* **94,** 153101 (2009).

72 Pei, Y., Lensch-Falk, J., Toberer, E. S., Medlin, D. L. & Snyder, G. J. High thermoelectric performance in PbTe due to large nanoscale Ag2Te precipitates and La doping. *Adv. Funct. Mater.* **21,** 241–249 (2011).